Study on Constraint Condition for Spectral Inversion Technique

T. Kanno
Kyushu University, Japan

J. Takeda
Kajima Corporation, Japan

15 WCEE
LISBOA 2012

SUMMARY:
As one of the techniques to evaluate the site effects, the spectral inversion technique is proposed. This technique has an advantage that the evaluation of site effects of many observation points is possible simultaneously, but has limitation to have to be given an appropriate constraint condition to arrive at a right solution. In this study, plural data set is constructed from records acquired at observation points of the K-NET, the KiK-net and the Seismic Intensity Information Network in Hiroshima prefecture, Japan, and the spectral inversion technique is applied to these data sets. And we also examined multiple constraint conditions to compare and discuss the results. As results, it is judged that the condition that the 1-D theoretical site amplification factors based on the underground structure model at five observation points are given is appropriate to evaluate the site effects.

Keywords: spectral inversion technique, site amplification factor, seismic motion records

1. INTRODUCTION

Seismic motions are known to be amplified significantly due to the effects of ground properties. Therefore, it is an extremely important aspect of earthquake disaster prevention measures to estimate these site effects with good precision.

One of the techniques for estimating these site effects is the spectral inversion technique (Iwata and Irikura, 1988) which separates the characteristics of seismic source, propagation path, and site effects on the basis of the Fourier spectra of observed seismic motions. This technique does not require extensive underground structure survey, and it is possible to assess simultaneously the site effects at multiple observation points. Moreover, it has an advantage in that it is not easily restricted by the conditions prevailing at the observation point. However, it requires constraint conditions to suppress any trade-off between the source characteristics and the site amplification characteristics. In a previous study (Iwata and Irikura, 1988), a constraint condition was established by specifying the site amplification characteristics to be twice the free surface characteristics by including bedrock observation points in the data set. However, it is not easy to select an ideal bedrock observation point.

In this study, we applied spectral inversion at seismic observation points in Hiroshima Prefecture to evaluate the site effects. We also examined multiple constraint conditions to compare and discuss the results.

2. RECORDS AND SUBJECT POINTS USED IN THE ANALYSIS

The subject observation points in this study were from K-NET, KiK-net (Okada *et al*., 2004), and the Seismic Intensity Information Network in Hiroshima Prefecture, Japan (a total of 134 points). The locations of the subject points are shown in Fig. 1. In our analysis, we used the records taken from these observation points, which satisfied the following conditions:

(1) Records made between January 2001 and May 2008 (records until December 2003 for those from the Seismic Intensity Information Network)
(2) Magnitudes of 4.0 or larger
(3) Peak ground acceleration of 200 gal or smaller
(4) Each earthquake is observed at a minimum of five different points.

To set the direct S wave as the subject of analysis, we used the waveforms for 5 s from the initial motion of the S wave read visually from the two components of horizontal motion as one sample. The analysis length for the Fourier spectra was set to 1024 data by adding some zeros after the sample. Fourier transformation was conducted on the two components of horizontal motion to calculate the Fourier spectra for horizontal motion using Eqn. 2.1.

$$FS = \sqrt{FS_{NS}^2 + FS_{EW}^2} \tag{2.1}$$

Here, FS_{NS} and FS_{EW} are the Fourier spectra of the NS component and the EW component of seismic motion observed on the ground surface, respectively. The subject frequency was set to 0.1-20 Hz.

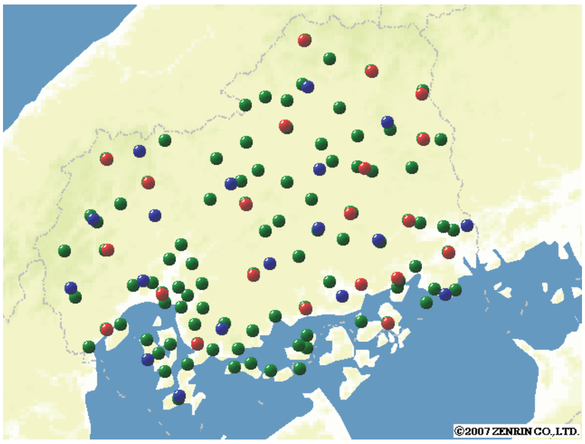

Figure 2.1. Locations of observation points used for analysis.

3. SPECTRAL INVERSION

3.1 Outline

In spectral inversion (Iwata and Irikura, 1988) it is supposed that the seismic motions of the S wave are a linear combination of source characteristics, propagation path characteristics, and site amplification characteristics. If I earthquakes are observed at all of the J observation points now, the seismic motion spectra O_{ij} for the i-th earthquake observed on the j-th observation point can be expressed as shown in Eqn. 3.1.

$$O_{ij}(f) = \frac{1}{R_{ij}} \times S_i(f) \times G_j(f) \times \exp\left(-\frac{\pi f R_{ij}}{Q_S V_S}\right) \tag{3.1}$$

Here, R_{ij} indicates the hypocentral distance of the i-th earthquake at the j-th observation point, S_i denotes the source characteristics of the i-th earthquake, G_j denotes the site amplification characteristics for the j-th observation point, and V_S and Q_S are the average S wave velocity and the Q value of the S wave for the propagation path, respectively. This model becomes true under the two assumptions that the seismic source spectra for a certain earthquake do not depend on the observation point and that the Q value does not depend on the propagation path. $I \times J$ pieces of equations become true with the combination of earthquake and observation point. Moreover, by solving this system of equations, I pieces of source characteristics, J pieces of site amplification characteristics, and one piece of Q value, for a total of $I+J+1$ pieces of parameters, are determined for each frequency. However, this does not have a unique solution as there is a trade-off relationship between S_i and G_j. We thus need a constraint condition to solve this. This condition needs to be determined carefully as it has a considerable influence on the results.

3.2 Constraint condition

In this study, we conducted spectral inversion using the following three constraint conditions, and we examined the estimation precision of each.

3.2.1. Constraint condition 1

Both surface and borehole records are obtained at KiK-net observation points. While the borehole records contain the effects of reflected waves, it is possible to use them to estimate the site amplification characteristics by removing them. In constraint condition 1, these estimated site amplification characteristics are applied to one of the KiK-net observation points as known data. The site amplification characteristics with the effects of reflected waves removed from the borehole records are calculated as follows:

First, the spectral ratio for the seismic motions observed both on the surface and in the borehole (H/H spectra) for all records obtained at the observation points is calculated using Eqn. 3.2.

$$H/H = \sqrt{FS_{NS}^2 + FS_{EW}^2} \Big/ \sqrt{FB_{NS}^2 + FB_{EW}^2} \tag{3.2}$$

Here, FS_{NS} and FS_{EW} indicate the Fourier spectra of the NS and EW components of the seismic motions observed on the surface, respectively, and FB_{NS} and FB_{EW} indicate the Fourier spectra of the NS and EW components of the seismic motions observed in borehole. Next, 10 samples with stable shapes are selected from all H/H spectra calculated for each observation point, and the average of these is considered the average *H/H* spectra for the observation point. Then the genetic algorithm (GA) (Yamanaka and Ishida, 1996) is used to obtain the underground structure model to satisfy these average *H/H* spectra. Finally, the site amplification factors without the effects of reflected waves are calculated based on the one-dimensional propagation theory from the identified underground structure model.

3.2.2. Constraint condition 2

In constraint condition 2, the site amplification factors calculated in the same way as constraint condition 1 are given to the five KiK-net observation points as known data.

3.2.3. Constraint condition 3

In constraint condition 3, the source characteristics for five observed earthquakes are given as known data by approximating it to the omega-square model (Aki, 1967) If the seismic source spectra follow the omega-square model, the seismic source spectra are expressed by Eqn. 3.3.

$$S(f) = \frac{\Omega_0 (2\pi f)^2}{1 + (f/f_C)^2} \tag{3.3}$$

Here, Ω_0 is expressed by Eqn. 3.4. f_C (Hz) is the corner frequency, which is calculated by Eqn. 3.5.

$$\Omega_0 = \frac{M_0 R(\theta, \phi)}{4\pi\rho V_S^3} \tag{3.4}$$

$$f_C = 4.9 \times 10^4 V_S \left(\frac{\Delta\sigma}{M_0} \right)^{1/3} \tag{3.5}$$

However, the radiation pattern coefficient here is supposed to be isotropic with $R(\theta, \phi) = 0.63$, density $\rho = 2.7$ g/cm^3, and S wave velocity $V_S = 3.4$ km/s. $\Delta\sigma$ is the stress drop (MPa), and we used $\Delta\sigma = 31$ MPa, which was the geometric average value of Sato (2003) for the stress drop in an intra-slab earthquake in the Philippine Sea Plate. M_0 is the seismic moment (Nm), and the value of the seismic mechanism solution by F-net (Okada *et al.*, 2004) is used. In addition, while Eqns. 3.3 and 3.4 are theoretical equations and need to have units with unified values, Eqn. 3.5 is an empirical equation for which the value in the previously described unit is acceptable.

Eqn. 3.3 has f_C as the boundary, and its shape becomes flat in frequency ranges higher than that. However, in reality, it exhibits a tendency to decrease in frequency ranges higher than the cut-off frequency f_{max}. Therefore, we made a correction in this study using a high cut filter P_S for small earthquakes by Tsurugi *et al.*(2006) This is expressed by Eqn. 3.6.

$$P_S(f) = \left\{ 1 + \left(\frac{f}{7.5} \right)^{2\times1.2} \right\}^{-1/2} \tag{3.6}$$

3.3 Preparation of the data set

We prepared an annual data set over the course of eight years using the records in Hiroshima Prefecture. The KiK-net observation point for which the site amplification characteristics are given as known data to be used as a reference observation point is the point where the site amplification characteristics value without the effects of reflected waves is the smallest in each data set under constraint condition 1. It was set to the five points with the smallest site amplification characteristics values under constraint condition 2. When constraint condition 3 was used, we used the source characteristics for five earthquakes considered to have happened within the Philippine Sea Plate as known data. Examples of theoretical calculation values of site amplification characteristics and source characteristics used in each of the constraint conditions are shown in Figs. 3.1 and 3.2.

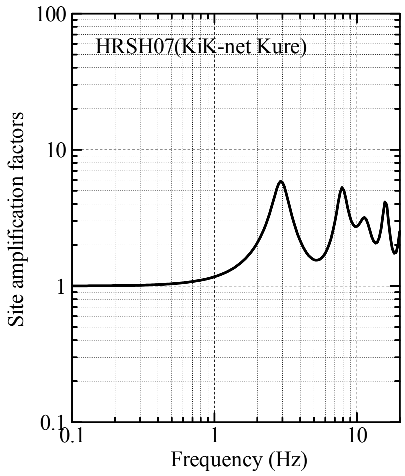

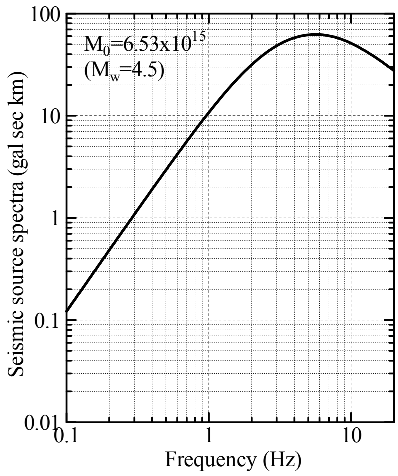

Figure 3.1. Theoretical site amplification characteristics (left figure).
Figure 3.2. Theoretical seismic source spectra (right figure).

3.4 Results

We conducted spectral inversion for each data set and considered the average value for each separated site amplification characteristics as the final result. As an example, the site amplification characteristics at HRSH01 (KiK-net Mihara) when each of the constraint conditions are used are shown in Fig. 3.3. In addition, the effects of reflections by the free surface are not included in these results.

First, when we compare the results corresponding to constraint conditions 1 and 2, the results corresponding to constraint condition 2 had smaller fluctuation within the data set, and the site amplification characteristics were estimated with stability. Comparing the results corresponding to constraint conditions 2 and 3, the shapes are similar on the high frequency range. However, for the site amplification characteristics obtained when constraint condition 3 is used, the amplification rate, which should gradually approach the value 1 theoretically at frequencies lower than 1 Hz, exceeded 1 greatly. One of the possible causes for this is the noise included in the observation records. Since such a tendency is observed for all observation sites in the analysis, there is likely to be an error caused by applying the omega-square model as a constraint condition instead of a characteristic unique to the observation point. In addition, results from constraint condition 2 were more stable with smaller fluctuations within each data set.

Next, Fig. 3.4 shows the source characteristics for an intra-slab earthquake with a moment magnitude M_w in the range 4.0-5.0 as an example of the source characteristics under each of the constraint conditions. It also shows the theoretical values for M_w = 4.0, 4.5 and 5.0 given by the omega-square model. When constraint condition 1 is used, there is a large trough around 3.5 Hz. Since this is observed in common for source characteristics when constraint condition 1 is used, it is suspected to be an effect of the condition. It also exhibits smaller values and larger fluctuations compared to the omega-square model. When the results corresponding to constraint conditions 2 and 3 are compared, they show a similar tendency for frequencies higher than approximately 0.8 Hz, but the results corresponding to condition 2 exhibit larger fluctuations. The resulting values tend to be larger than the theoretical values in the low-frequency range when condition 2 is used, which seems to be an effect of the noise contained in the records themselves. There is a tendency for the source characteristics to have larger fluctuations when the site amplification characteristics are used as a constraint condition, and for the site amplification characteristics to have larger fluctuations when the source characteristics are used as a constraint condition. This is due to the above-mentioned trade-off relationship between the source characteristics and the site amplification characteristics.

Finally, the Q value, which corresponds to the propagation path characteristics when each of the constraint conditions is used, is shown in Fig. 3.5. The distribution of the Q value reveals a similar tendency regardless of the constraint condition, and its fluctuation is rather large around 1 Hz. A separate and more detailed examination would be necessary to determine the cause of the fluctuation by considering the type of earthquake, regional differences in source location, and so forth.

Due to the fact that the purpose of this study was to understand the site effects at each observation point, and that the fluctuation in the characteristics used as the constraint condition and the tendency of the Q value do not vary much between constraint conditions 2 and 3, we concluded in this study that the results corresponding to constraint condition 2 were the most reasonable.

The site amplification characteristics values estimated at HRS001 (K-NET Takano), HRSH01 (KiK-net Mihara), and HRSS01 (Seismic Intensity Information Network, Naka-ku, Hiroshima City) by using the constraint condition 2 are shown in Fig. 3.6. For K-NET and KiK-net observation points, the site amplification characteristics values of Nozu and Nagao (2005) are also shown. For reference, the subject frequency used by Nozu and Nagao (2005) was in the range 0.2-10 Hz. Their spectral inversion applied the point where the site amplification characteristics became smallest in each frequency based on preliminary analysis as the reference observation point to specify the site amplification characteristics of that point to be 1 as the constraint condition. In addition, they used a fixed Q value. It is thus impossible to make a direct comparison of the site amplification factor with this study. However, the shapes including the peak position are in good agreement for both HRS001 and HRSH01. Based on this, the site amplification characteristics estimated in this study appear to be valid. We also concluded that the number of earthquake records used in the analysis was sufficient and the estimation accuracy was reliable for HRSS01, although the number was smaller than that for HRS001 or HRSH01.

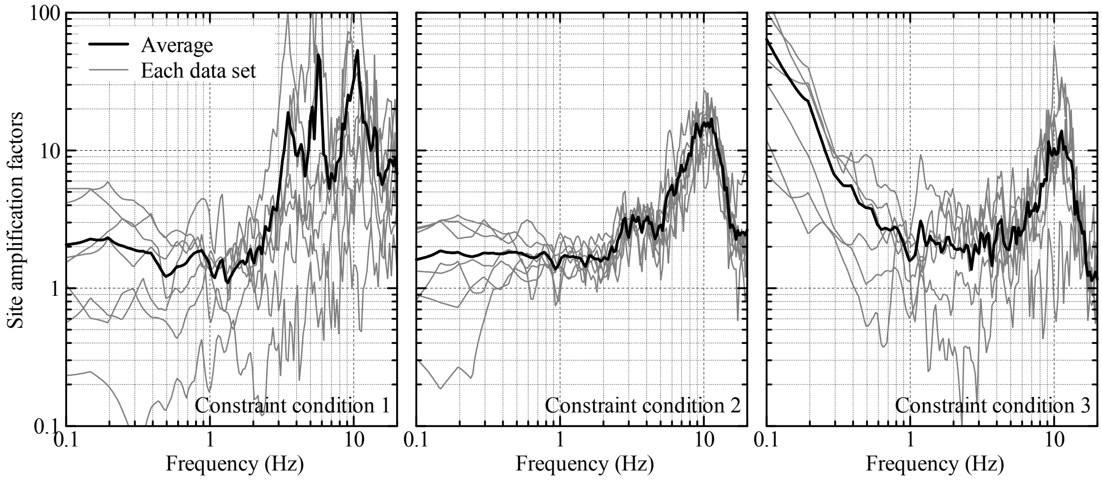

Figure 3.3. Difference in site amplification characteristics depending on the constraint condition.

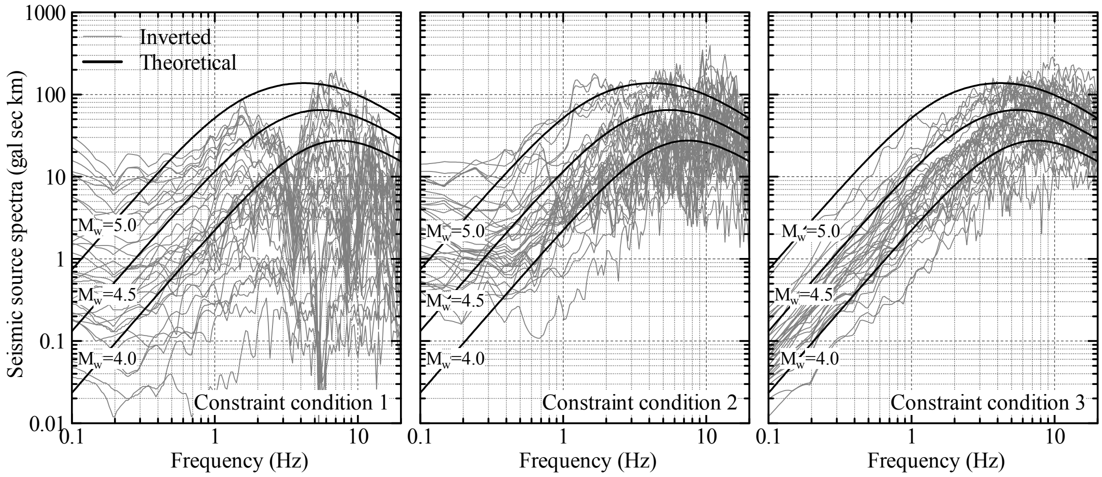

Figure 3.4. Difference in source characteristics depending on the constraint condition.

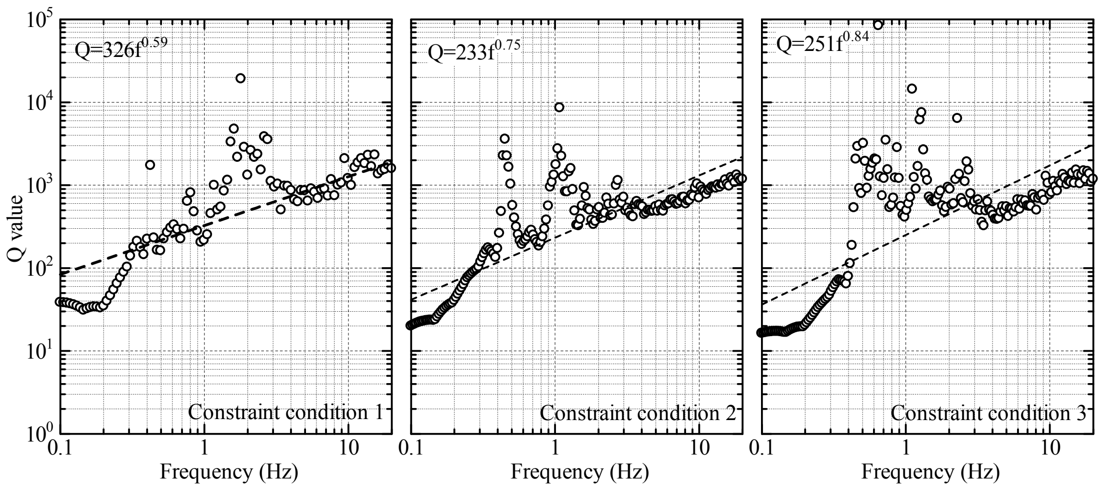

Figure 3.5. Difference in Q value depending on the constraint condition.

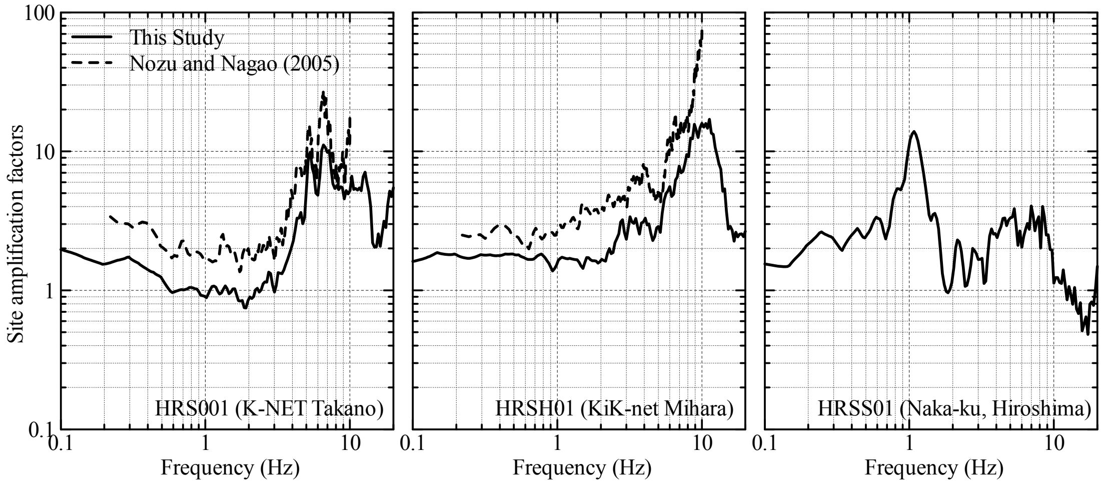

Figure 3.6. Comparison with the site amplification characteristics from Nozu and Nagao (2005).

4. ESTIMATED SITE AMPLIFICATION FACTOR

We prepared an illustration of the distribution of the average site amplification factor by utilizing the estimated site amplification characteristics and classifying the average site amplification factor to three types of "5 or smaller," "larger than 5 and equal to or smaller than 10," and "larger than 10" for two period ranges: a period range of 0.1-0.5 s that includes the dominant period for many observation points, and a period range of 0.5-1.0 s that is associated with moderate damage in general low-rise buildings (Sakai *et al.*, 2004) The results are shown in Fig. 4.1. The average site amplification factor is relatively small in mountainous areas, and there are points in coastal areas where the average site amplification factor exceeds 10. Since the average value of the site amplification factor exceeds 10 in areas with large populations including Hiroshima City and Kure City in the period range of 0.5-1.0 s, it is possible that damages may occur in cases of large earthquakes in the future. Due caution will be necessary.

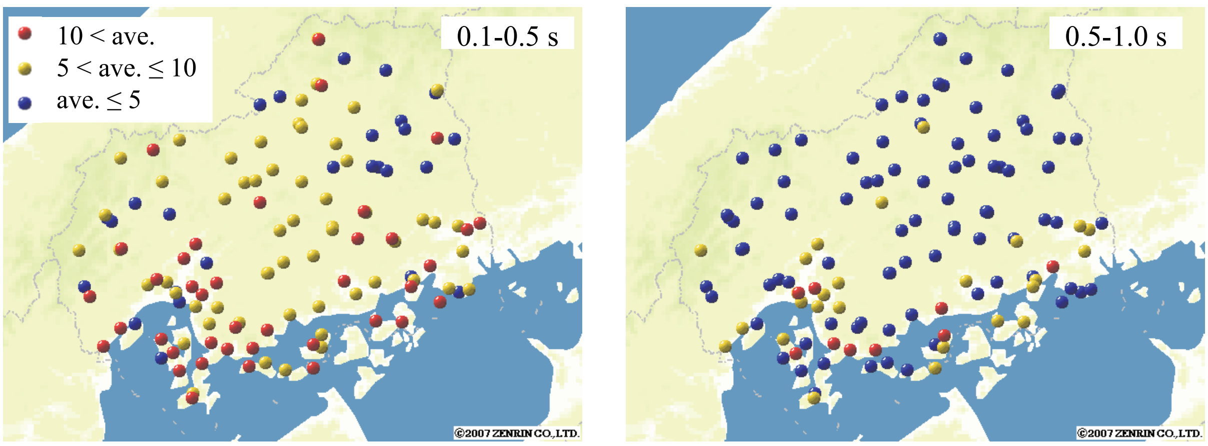

Figure 4.1. Distribution of average amplification factor for estimated site amplification characteristics.

5. CONCLUSIONS

In this study, we conducted spectral inversion by using three different constraint conditions to evaluate the site amplification characteristics at earthquake observation points in Hiroshima Prefecture. We also examined the accuracy of the estimations. Our findings are summarized as follows:

(1) When the site amplification characteristics that did not include the effects of reflected waves were applied to one observation point of KiK-net as a constraint condition, the estimated source characteristics and site amplification characteristics revealed large fluctuations in each data set.
(2) When the site amplification characteristics that did not include the effects of reflected waves were applied to five observation points of KiK-net as a constraint condition, the estimated site amplification characteristics revealed little fluctuation in each data set.
(3) When the source characteristics that followed the omega-square model were applied to five earthquakes as a constraint condition, the site amplification characteristics revealed moderate fluctuation within the data set, although the estimated source characteristics were close to the theoretical values.
(4) The site amplification characteristics were estimated with the highest precision when the characteristics that did not include the effects of reflected waves were given to five observation points of KiK-net as a constraint condition.
(5) The site amplification characteristics eventually adopted were in good agreement with the existing study results, and the site amplification characteristics obtained in this study appear to be valid.
(6) There was a tendency for the estimated site amplification factor to be smaller for observation points in mountainous areas and larger for observation points in the coastal areas.

AKCNOWLEDGEMENT
The seismic records used in this study were observed by K-NET and KiK-net run by the National Research Institute for Earth Science and Disaster Prevention, and the Seismic Intensity Information Network in Hiroshima Prefecture. We hereby express our gratitude to all related parties.

REFERENCES

Iwata, T. and Irikura, K. (1988). Source parameters of the 1983 Japan-Sea earthquake sequence, *J. Phys. Earth*, **36**, 155-184.

Okada, Y., Kasahara, K., Hori, S., Obara, K., Sekiguchi, S., Fujiwara, H. and Yamamoto, A. (2004). Recent progress of seismic observation networks in Japan: Hi-net, F-net, K-NET and KiK-net, *Earth, Planets and Space*, **56**, 15-28.

Yamanaka, H. and H. Ishida (1996). Application of Genetic Algorithms an Inversion of Surface-Wave Dispersion Data, *Bull. Seismological Society of America*, **86:2**, 436-444.

Aki, K. (1967). Scaling law of seismic spectrum, *J. Geophys. Res.*, **72**, 1217-1231.

Satoh, T. (2003). Relation of stress drops of small and moderate earthquakes to focal mechanism, fault type, focal depths, and regions, *JSCE Journal of Earthquake Engineering*, **24:48**, 1-8 (in Japanese with English abstract).

Tsurugi, M., Kagawa, T., Okazaki, A., Hada, K. and Irikura, K. (2006). Study on a high-cut filter for strong ground motion prediction - Based on the observed records during the 1995 Hyogo-ken Nambu Earthquake -, Journal of Japan Association for Earthquake Engineering, 6:4, 94-112 (in Japanese with English abstract).

Nozu, A and Nagao, T. (2005). Simulation of strong motions from shallow crustal and subduction-zone earthquake based on site-specific amplification and phase characteristics, *Technical note of the Port and Airport Research Institute*, **1112**, 1-56 (in Japanese with English abstract).

Sakai, Y., Kanno, T. and Koketsu, K. (2004). Proposal of instrumental seismic intensity scale from response spectra in various period ranges, *Journal of structural and construction engineering*, **585**, 71-76 (in Japanese with English abstract).